Solar panel technologies for light-to-chemical conversion

Virgil Andrei, Qian Wang, Taylor Uekert, Subhajit Bhattacharjee, Erwin Reisner*

Yusuf Hamied Department of Chemistry, University of Cambridge, Lensfield Road,
Cambridge CB2 1EW, United Kingdom.
*Correspondence to: reisner@ch.cam.ac.uk. Website: www-reisner.ch.cam.ac.uk.

Conspectus

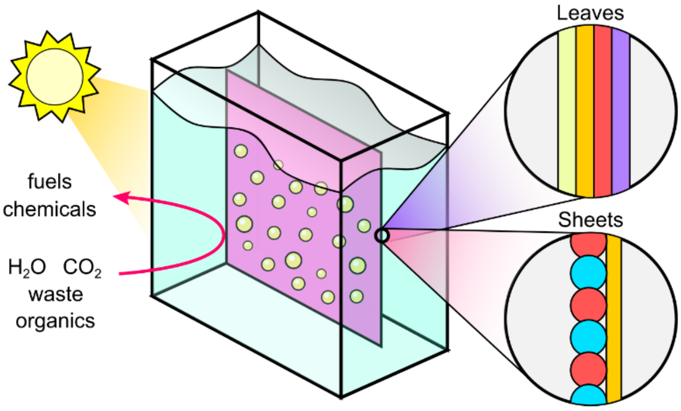

The sustainable synthesis of fuels and chemicals is key to attaining a carbon neutral economy. This can be achieved by mimicking the light harvesting and catalytic processes occurring in plants. Solar fuel production is commonly performed via established approaches, including photovoltaic-electrochemical (PV-EC), photoelectrochemical (PEC), and photocatalytic (PC) systems. A recent shift saw these systems evolve into integrated, compact panels, which suit practical applications through their simplicity, scalability and ease of operation. This advance has resulted in a suite of apparently similar technologies, including the so-called artificial leaves, PC sheets and panels. In this Account, we compare these different thin film technologies based on their micro- and nanostructure (i.e. layered vs. particulate), operation principle (products occurring on the same or different sides of the panel), and product/reaction scope (overall water splitting and CO_2 reduction, or organics, biomass and waste conversion).

For this purpose, we give an overview of developments established over the past five years in our laboratory. Two light absorbers are generally required to overcome the thermodynamic challenges of coupling water oxidation to proton or CO_2 reduction with good efficiency. Hence, tandem artificial leaves combine a lead halide perovskite photocathode with a $BiVO_4$ photoanode to generate syngas (a mixture of H_2 and CO), whereas PC sheets involve metal-ion-doped $SrTiO_3$ and $BiVO_4$ particles for selective formate synthesis from CO_2 and water. On the other hand, only a single light absorber is required for coupling H_2 evolution to organics oxidation in the thermodynamically less demanding photoreforming process. This can be performed by immobilized carbon nitride (CN_x) in case of PC panels, or by a single perovskite light absorber in the case of PEC reforming. Such systems can be integrated with a range of inorganic, molecular and biological catalysts, including metal alloys, molecular cobalt complexes, enzymes, or bacteria, with low overpotentials and high catalytic activities towards selective product formation.

This wide reaction scope introduces new challenges towards quantifying and comparing the performance of different systems. To this end, we propose new metrics to evaluate the performance of solar fuel panels, based on the areal product rates and commercial product value. We further explore the key opportunities and challenges facing the commercialization of thin film technologies for solar fuels research, including performance losses over larger areas and catalyst/device recyclability. Finally, we identify emerging applications beyond fuels, where such light-driven panels can make a difference, including waste management, chemical synthesis, and pharmaceutical industries. In the long term, these aspects may facilitate a transition toward a light-driven, circular carbon economy.

Key References

- Andrei, V.; Reuillard, B.; Reisner, E. Bias-free solar syngas production by integrating a molecular cobalt catalyst with perovskite–$BiVO_4$ tandems. *Nat. Mater.* **2020**, *19*, 189–194.[1] *Demonstration of an unassisted perovskite–$BiVO_4$ PEC artificial leaf. An integrated perovskite photocathode enables the device to couple O_2 evolution to the challenging aqueous CO_2 reduction.*

- Wang, Q.; Warnan, J.; Rodríguez-Jiménez, S.; Leung, J. J.; Kalathil, S.; Andrei, V.; Domen, K.; Reisner, E. Molecularly engineered photocatalyst sheet for scalable solar formate production from carbon dioxide and water. *Nat. Energy* **2020**, *5*, 703–710.[2] *A molecular cobalt catalyst integrated on a wireless, monolithic photocatalyst sheet based on $SrTiO_3$:La,Rh and $BiVO_4$:Mo particles, enabling selective solar-driven CO_2-to-formate conversion coupled with water oxidation.*

- Uekert, T.; Bajada, M. A.; Schubert, T.; Pichler, C. M.; Reisner, E. Scalable Photocatalyst Panels for Photoreforming of Plastic, Biomass and Mixed Waste in Flow. *ChemSusChem* **2021**, *14*, 4190–4197.[3] *Immobilized CN_x panels produce H_2 and oxidize waste under flow during solar irradiation, overcoming the recyclability challenge of particulate systems.*

- Bhattacharjee, S.; Andrei, V.; Pornrungroj, C.; Rahaman, M.; Pichler, C. M.; Reisner, E. Reforming of Soluble Biomass and Plastic Derived Waste Using a Bias-Free $Cu_{30}Pd_{70}$|Perovskite|Pt Photoelectrochemical Device. *Adv. Funct. Mater.* **2021**, 2109313.[4] *A PEC leaf employing a single perovskite light absorber demonstrates selective biomass and PET reforming while producing H_2 at rates higher than conventional PC approaches.*

1. Introduction

While renewable electricity is becoming more widespread, aviation, shipping and the chemical industries still rely heavily on conventional fuels. Hence, solar-driven chemical synthesis will become a crucial contributor to attaining a circular economy. Solar fuel production has been pursued ever since the initial studies on solar water splitting on TiO_2 photoelectrodes by Fujishima and Honda fifty years ago.[5] Since then, PV-EC, PEC and PC systems stood out as the most common alternatives for solar-to-chemical conversion.[6] However, overall fuel production limits the choice of single light absorbers to wide bandgap semiconductors absorbing mainly in the UV range.[5,7] Hence, many studies only focused on photoelectrodes and photocatalyst powders with sacrificial reagents for either proton/CO_2 reduction or water oxidation.[8]

Complementary light absorbers can be combined to attain a higher coverage of the visible spectrum, with early multi-junction systems already reaching a 18.3% efficiency for overall water splitting in 2000.[9] Such light harvesters can also be interfaced directly or indirectly to biologic systems like bacteria, producing organics at efficiencies beyond 4% which exceeds natural photosynthesis.[10,11] However, this approach requires a more complex wiring and reactor design in the case of PV-EC systems and photoelectrodes,[12] as well as a careful choice of redox mediators for PC suspensions,[13,14] thereby limiting their implementation to laboratory prototypes.

Over the past decade, these three distinct technologies began undergoing the next stage of development, evolving towards integrated, compact systems that are more suitable for wider applications. By removing wiring, thin film light absorbers could be interfaced directly with suitable electrocatalysts to form the well-known "artificial leaves", a term introduced in 2011.[15,16] On the other hand, practical PC water splitting could be demonstrated by immobilizing semiconductor particles onto a thin solid conductive film (Figure 1), as reported in 2016.[17,18]

In this Account, we distil the common design principles of such thin film technologies including artificial leaves consisting of multiple thin layers of materials and photocatalyst sheets containing a layer of semiconductor particles, assessing their individual prospects and challenges for solar fuel production, and proposing alternative performance metrics. On this occasion, we summarize our recent progress in expanding the scope of these technologies beyond H_2 production and discuss solar chemical applications more broadly. In addition, we showcase oxidative organic transformations including biomass[19,20] or plastic[21] photoreforming as a way to circumvent the thermodynamic limitations imposed by water oxidation, and explore how this can be expanded to flat panel systems.

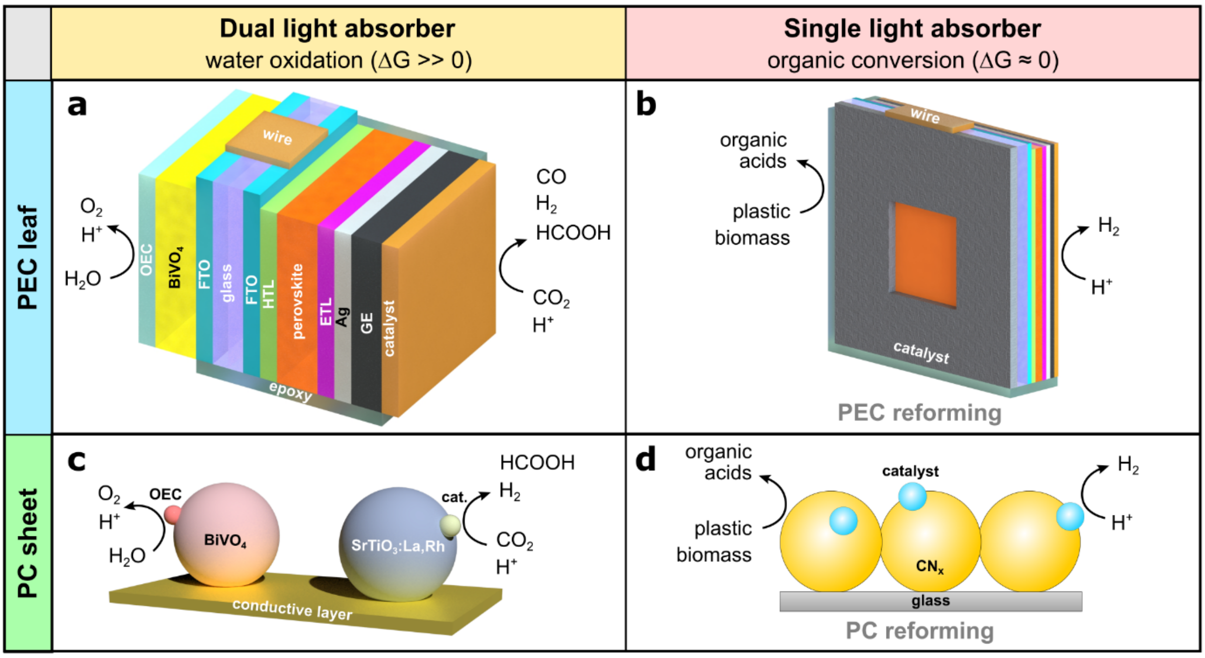

Figure 1. Examples of standalone thin film technologies described in this Account: (a,b) PEC artificial leaves, (c,d) PC sheets. (a) A tandem $BiVO_4$ – perovskite tandem device can produce O_2 and syngas (H_2 + CO) or formate from water and CO_2. (b) A single perovskite light absorber performs simultaneously proton reduction and organics oxidation. The perovskite PV device structure corresponds to the one in (a), but the $BiVO_4$ photoanode is replaced by a metal alloy electrocatalyst. (c) Doped $BiVO_4$ and $SrTiO_3$ powders are interfaced through a solid gold layer, achieving hydrogen or selective formate production. (d) Immobilized semiconductor particles combine H_2 evolution with reforming of organics. Abbreviations: OEC – oxygen evolution catalyst; FTO – fluorine-doped tin oxide; HTL/ETL – hole/electron transport layer; GE – graphite epoxy paste (conductive encapsulant); CN_x – carbon nitride.

2. Thin film technologies

Solar fuels can be produced using a wide range of configurations, which makes an unequivocal classification of those systems challenging. While several nomenclatures have already been reported for solar fuels systems,[22,23] we propose a simple classification based on the oxidation reaction and device structure. The distinct thermodynamic requirements of organic oxidation and O_2 evolution may demand a single or tandem light absorber configuration, whereas the starting material could be more suitable for a layered or particulate panel.

2.1. Water oxidation coupled to H^+/CO_2 reduction

2.1.1. Artificial leaves

The “artificial leaf” design was experimentally demonstrated by Nocera in 2011, by sandwiching a triple-junction amorphous silicon solar cell between NiMoZn and Co-based catalysts.[15,16] Ever since, a broad community has started developing integrated devices,[24] expanding this concept to a wide range of light absorbers in PEC or PV-PEC configurations. Despite solar-to-hydrogen conversion efficiencies reaching beyond 3% for water splitting (Table 1),[25] CO_2 reduction posed challenges for artificial leaf devices using only two light absorbers. This occurred as most conventional narrow bandgap light absorbers (such as Si, Cu_2O, or dyes) provide photovoltages below 0.7 V,[26] whereas an additional overpotential of ~0.4 V must be overcome for commonly employed CO production catalysts. Instead, several studies focused on the CO_2 reduction to formate, which could be accomplished at low overpotentials using tandem $SrTiO_3$ – InP[27] and triple-junction amorphous SiGe[28] leaves.

Our laboratory could overcome these challenges by introducing lead-halide perovskite photocathodes, which were combined with $BiVO_4$ photoanodes in back-to-back, two-electrode tandem PEC devices (Figure 1a).[1,29] In this arrangement, a buried-PV electrode was constructed by encapsulating a perovskite PV cell with a conductive layer (either Field's metal,[1,29] or graphite epoxy paste[30,31]), which provided an interface to molecular and inorganic electrocatalysts with low overpotentials towards CO_2 reduction. The thin graphite paste encapsulation enabled a redesign of the device structure, resulting in lightweight artificial leaves which stand out in terms of cost, scalability and functionality. [32] This arrangement could be expanded to semi-artificial photosynthesis systems interfacing semiconductors to enzymes with very low overpotentials for proton or CO_2 reduction.[33–35] By integrating hydrogenase in a hierarchically structured inverse opal TiO_2 scaffold, such systems could perform water splitting at 1.1% solar-to-hydrogen efficiency,[34] whereas a 0.8% solar-to-formate efficiency and a Faradaic yield of 83% were attained with formate dehydrogenase.[33]

2.1.2. PC sheets

Particulate photocatalysts can also be used to produce solar fuels from water and CO_2. In such processes, the reduction and oxidation reactions typically take place in close proximity to one another using redox mediators, preventing concentration overpotentials and avoiding the use of an electrolyte.[7] To ensure adequate mass transfer, photocatalytic processes are typically carried out by dispersing the photocatalyst powder in a reaction solution. While a powder suspension is the simplest way to generate solar fuels, it has several disadvantages in terms of recycling and large-scale applications. One strategy for tackling these issues is to fabricate a photocatalyst sheet by fixing the photocatalyst powder on a substrate.[36,37] A recent milestone demonstrated a 100 m^2 array of Al-doped $SrTiO_3$ photocatalyst sheets that generated solar H_2 over several months via water splitting, showing a maximum solar-to-hydrogen conversion efficiency of 0.76%.[38]

Additionally, photocatalytic processes can be accomplished by employing a nature-inspired Z-scheme configuration, consisting of two distinct photocatalysts connected by a redox mediator for interparticle electron relay. Z-scheme photocatalyst sheets (Figure 1c) comprise two photocatalysts embedded in a conductive layer, such as gold or carbon, to ensure interparticle electron transfer while avoiding the side reactions caused by redox mediators.[17,18] One example is a photocatalyst sheet containing $SrTiO_3$:La,Rh and $BiVO_4$:Mo that is fixed on a Au layer and achieves a solar-to-hydrogen conversion efficiency of above 1%.[17]

Light-driven fuel production from CO_2 is currently hampered by sacrificial electron donor utilization, low efficiency, selectivity and scalability. To overcome these barriers, our laboratory integrated a selective molecular catalyst (phosphonated cobalt(II) bis(terpyridine) catalyst, CotpyP) on semiconductor light absorbers to form a wireless, monolithic photocatalyst sheet (CotpyP-$SrTiO_3$:La,Rh|Au|$BiVO_4$:Mo).[2] The device combines the high selectivity of molecular catalysts for CO_2 reduction and the strong water oxidation ability of semiconductors, resulting in a solar-to-formate conversion efficiency of 0.08±0.01% with a selectivity for formate of 97±3%. Furthermore, our laboratory developed an approach to produce multicarbon products by combining photocatalyst sheets ($SrTiO_3$:La,Rh|ITO|$BiVO_4$:Mo) capable of photocatalytic water splitting with the nonphotosynthetic, CO_2-fixing acetogenic bacterium *Sporomusa ovata* as a living biocatalyst. The resulting bio-abiotic hybrid system combines the light-harvesting ability of the photocatalyst sheet with the high selectivity of the biological catalyst, thereby achieving a solar-to-acetate conversion efficiency of ~0.7% with high selectivity for acetate production.[39]

2.2. Organics oxidation coupled to H^+/CO_2 reduction

Coupling water or CO_2 reduction with the oxidation of organic substrates can lower the required potential to near-neutral levels, while also promoting the potential formation of useful organic products. Waste streams such as plastics, biomass, food, or mixed municipal solids are particularly desirable substrates as they contain oxidizable organic molecules of the form $C_xH_yO_z$, are freely available, and require creative mitigation solutions.[40]

2.2.1. Artificial leaves

There have been a few reports on 'two-compartment' PEC systems for H_2 evolution, which utilize simple organic substrates such as glucose[41–43] or glycerol[44–46] instead of water oxidation. However, most of those PEC systems either require an additional external energy input in the form of applied bias,[41,43–45] employ a tandem light absorber configuration,[42,47] or exhibit low efficiencies and product selectivities.[41–43,46,47] Furthermore, a 'two-compartment' arrangement may be impractical for large scale applications.

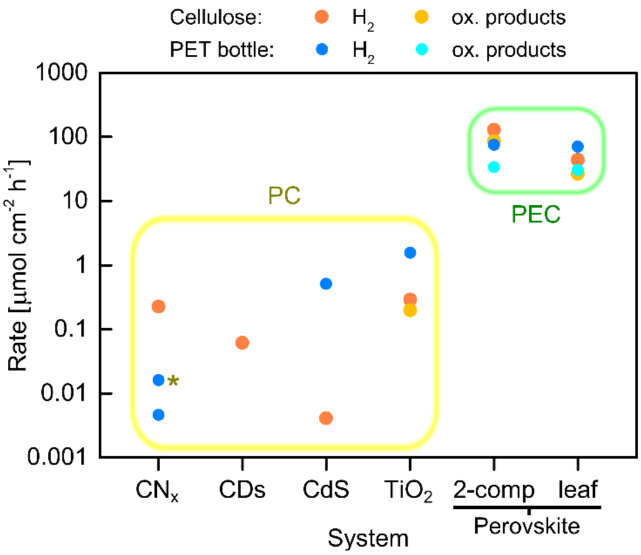

Figure 2. Comparison between the product rates of suspension and thin film technologies for photoreforming. Waste conversion can be performed with semiconductor particles (that is, PC reforming) or with integrated artificial leaves (PEC reforming). The star indicates a PC panel. CDs – carbon dots; PET – polyethylene terephthalate. Adapted with permission from ref. 4. Copyright 2022 the Authors. Published by Wiley under a Creative Commons Attribution 4.0 International (CC BY 4.0) License.

We have recently developed a single-light absorber PEC device which can reform a diverse range of pre-treated waste substrates and simultaneously generate H_2. These $Cu_{30}Pd_{70}$|perovskite|Pt leaves integrate a perovskite photocathode with a $Cu_{30}Pd_{70}$ anode (Figure 1b). The devices can convert glycerol (byproduct from the biofuel industry), polyethylene terephthalate (PET) bottles and cellulose (component of lignocellulosic biomass) into value-added products such as glyceric, glycolic and gluconic acid, with a product selectivity between 60-90%.[4] These bias-free PEC systems achieve 10^2-10^4 times higher product formation rates over conventional waste photoreforming approaches based on particulate photocatalysts (Figure 2). Another important aspect of this system is its versatility in terms of assembly. The PEC device can be constructed in either a two-compartment configuration, or as a standalone artificial leaf. The former is suitable for non-transparent waste streams, whereas the latter allows for facile device retrieval and reuse.

2.2.2. PC sheets

As with PEC systems, the application of photocatalyst sheets to simultaneous H_2 production and organic oxidation remains limited. This can be attributed to several challenges, including reduced mass transfer between the catalyst and reactant, parasitic light absorption by the reactant, and practical deposition difficulties. Nevertheless, a variety of TiO_2 sheets have been applied to photodegradation of organic pollutants.[48] H_2 generation with a triethanolamine electron donor was also reported with PC sheets prepared by drop-casting mesoporous CN_x coupled with a Pt co-catalyst onto stainless steel with a Nafion binder.[49] Recently, we have utilized a similar drop-casting technique to prepare $CN_x|Ni_2P$ sheets up to 5 × 5 cm^2 (Figure 1d). By illuminating these PC sheets from behind, this system was able to successfully photoreform turbid PET, biomass and mixed municipal waste streams into H_2 and various small organics such as formate, carbonate, and glyoxal.[3] $CN_x|Pt$ and $TiO_2|Pt$ sheets prepared by the same strategy were also shown to produce H_2, ethane, and ethylene from polyethylene-derived organic acids.[50]

3. Assembly and characterization

3.1. Assembly

As a key common feature, these thin film technologies take the shape of a compact panel, where the precise assembly of the light harvesting and catalytic components governs the reactivity. To prepare an artificial leaf, the individual components of an unassisted PV-EC or PEC system must be integrated in a standalone device. Such devices can be fabricated in a wireless, monolithic design, where the catalysts are interfaced to both sides of the light harvester.[15,28] The same functionality can be obtained by attaching a photocathode to a suitable (photo)anode in a back-to-back, tandem device configuration.[29] In this case, the front electrode (typically a wide bandgap photoanode) needs to be partially transparent, while the connection between both electrodes is made through a short, embedded wire.[1] Those individual photoelectrodes can be fabricated by conventional deposition techniques including spin coating, electrodeposition, drop casting, or thermal evaporation.[29,51]

Transitioning from powder suspensions to PC sheets requires immobilization of the particles onto a substrate. This may require further post-annealing treatment, binders, and textured substrates like frosted glass[3,38] to increase the photoactive area and improve semiconductor adhesion. If two different light absorber particles are used, a conductive interface is also necessary. This can be provided by thermal evaporation of a Au[2,17] or carbon layer,[18] or addition of indium tin oxide (ITO)[52] nanoparticles. In the case of overall water splitting, care must be taken to prevent the backward reaction (O_2 reduction and H_2 oxidation), as H_2 and O_2 are produced in close vicinity. This can be prevented by photodeposition of Cr_2O_3 and TiO_2 surface modifiers. The hydrated oxide layers hinder O_2 penetration, while allowing protons to reach the catalytic centers for H_2 production.[17]

3.2. Characterization and product quantification

Prior to the assembly of bias-free, two-electrode PEC systems or standalone artificial leaves, the respective cathodic and anodic processes should be thoroughly analyzed to determine the exact operating conditions (working potentials and expected current densities) during unassisted operation. For this purpose, cyclic voltammetry (CV) scans of the individual (photo)electrodes must be taken in a two-compartment, three-electrode setup, where Ag/AgCl and Pt can act as reference and counter electrodes. The overlap between the individual CV scans of the (photo)anode and (photo)cathode corresponds to the ideal current density during bias-free operation of the artificial leaf. This overlap also determines the potential applied on the catalysts during operation; hence, the product selectivity can be steered by adjusting the photovoltage and catalyst overpotential. For wired PEC devices, chronoamperometry is performed under simulated sunlight irradiation (often AM 1.5G, 100 mW cm^{-2}) at zero applied bias voltage to determine the long-term performance of the system. In contrast, the performance is mainly evaluated by tracking the amounts of products for standalone artificial leaves (where both electrodes are directly connected) and PC sheets.

Depending on the choice of substrates and reaction, a diverse range of products can be generated from PEC artificial leaves and PC sheets. Gaseous products such as H_2, syngas or O_2 accumulate in the headspace of the reactor with time. These can be detected and quantified using gas chromatography either in-line, or through manual injection of a specific volume from the headspace. On the other hand, liquid products produced from the oxidation of waste substrates (e.g., formic acid, glycolic acid, glyceric acid) or CO_2 reduction (e.g., formate, acetate, alcohols) can be analyzed using a combination of high performance liquid chromatography, ion chromatography and NMR spectroscopy.

4. Performance metrics

Artificial photosynthesis systems are commonly evaluated by their solar-to-fuel conversion efficiency (η_{STF}), which can be calculated using formula (1), where $r_{product}$ is the product rate, ΔG is the reaction's Gibbs free energy ($\Delta G > 0$), P is the total incident solar power and A is the irradiated area.[8]

$$\eta_{STF} = \frac{r_{product}\ (mmol\ s^{-1}) \times \Delta G\ (J\ mol^{-1})}{P\ (mW\ cm^{-2}) \times A\ (cm^{2})} \tag{1}$$

In case of PEC systems, η_{STF} can be expressed as shown in formula (2), where J is the photocurrent density, FY is the Faradaic yield and ΔE is the applied voltage bias between the two electrodes. This voltage difference amounts to 1.23 V for water splitting, and 1.33 V when coupling water oxidation to CO production at 298 K.[53]

$$\eta_{STF} = \frac{J\ (mA\ cm^{-2}) \times FY \times \Delta E\ (V)}{P\ (mW\ cm^{-2})} \tag{2}$$

A comparison between solar fuel systems only by η_{STF} poses challenges when considering photocatalysis processes with a negative Gibbs free energy ($\Delta G < 0$).[54] As shown above, ΔG is mainly dependent on water oxidation, meaning that the η_{STF} value can be high for water and CO_2 splitting ($\Delta G >> 0$), while the η_{STF} of organic conversions will be per definition low ($\Delta G \approx 0$). However, some products are more valuable than others. Hence, as we expand the chemistry scope toward more complex oxidation reactions, the η_{STF} does not reflect the true economic value of a solar chemical process. To address this, we propose a number of alternative metrics for solar fuel production, which take the economic value of products into account. These metrics focus on the areal performance instead of the solar energy conversion efficiency.

A first general metric is the amount of product ($n_{product}$) synthesized per area (A) and time (t), which corresponds to the rate of conversion per area ($r_{product}$).

$$r_{product} = \frac{n_{product}\ (\mathrm{\mu mol})}{A\ (\mathrm{cm}^2) \times t\ (\mathrm{h})} \tag{3}$$

This can form the basis for other value-oriented metrics. A simplified solar-to-value (STV) creation rate can be obtained by subtracting the total value of substrates ($\sum_{j=1}^{m} C_j \times n_{j,substrate}$) from the value of products ($\sum_{i=1}^{n} C_i \times n_{i,product}$), as shown in equations (4) and (5) where C_i is the cost of a chemical *i*. This STV metric can be further expanded to include the cost of substrate pre-treatment, product separation, storage, other process costs and factor for scale, although calculating such values will require an extensive technoeconomic analysis. In the long term, such metrics may also consider the levelized cost of chemicals (analogous to the levelized cost of energy), measuring the average net value of chemicals for a solar plant over its lifetime.

$$STV = \frac{\sum_{i=1}^{n} C_i\ (\$\,\mathrm{mol}^{-1}) \times n_{i,product}\ (mol) - \sum_{j=1}^{m} C_j\ (\$\,\mathrm{mol}^{-1}) \times n_{j,substrate}\ (mol)}{A\ (\mathrm{cm}^2) \times t\ (\mathrm{h})} \tag{4}$$

$$STV = \sum_{i=1}^{n} C_i\ \ (\$\,\mathrm{mol}^{-1})\ \times\ r_i\ (\mathrm{mol\ cm}^{-2}\ h^{-1}) - \sum_{j=1}^{m} C_j\ \ (\$\,\mathrm{mol}^{-1})\ \times\ r_j\ (\mathrm{mol\ cm}^{-2}\ h^{-1}) \tag{5}$$

These metrics are particularly suitable for organic transformations, as the conversion rate is only limited by the photocurrent or light absorption of the semiconductor, which are determined by its external quantum efficiency (EQE) over the visible spectrum.[4] Moreover, the value of waste and CO_2 can be negative due to tipping fees and carbon taxes, respectively, meaning that value is created from both substrates (waste mitigation) and products (H_2, CO, organics). As the prices of chemicals fluctuate, value-driven metrics should be updated in dedicated databases, while the areal conversion rates would constitute fixed reported values.

From this point of view, PEC reforming would stand out when compared to its PC analogues, and would even approach the performance of state-of-the-art wired PV-EC systems for overall water splitting.[55] In our case, the product rates of perovskite artificial leaves for waste PEC reforming were improved 5-10 times over the perovskite-$BiVO_4$ devices for water splitting, and >3000 times over the photocatalytic CN_x panels for PET reforming, as shown in Table 1.[4]

Table 1. Performance metrics for some representative solar fuel systems (PV estimate given for comparison). Abbreviations: jn – junction; a – amorphous; KB_i – potassium borate buffer; CC – carbon cloth; RuCP – Ru complex polymer; PVK – perovskite; n.a. – not applicable.

Sample	η_{STF} (%)	Product	Product rate (µmol cm^{-2} h^{-1})	Value rate (\$ cm^{-2} h^{-1})	Comments	Ref.
Artificial leaves						
Co|3jn-a-Si|NiMoZn	2.5	H_2, O_2			0.5 M KB_i, 1.5 M KNO_3	15
IrO_x|3jn-a-SiGe|CC|RuCP	4.6	HCOOH (O_2)	59.7	$1.32\cdot10^{-6}$	CO_2 sat. 0.1 M KP_i, pH 6.4	28
Mo:$BiVO_4$ – PVK – Pt	3	H_2	41.9	$2.57\cdot10^{-7}$	0.1 M $KHCO_3$, pH 7	25
		O_2	22.0			
$BiVO_4$ – PVK|FM|CoMTPP@CNT	0.018	CO	0.18	$5.14\cdot10^{-9}$	0.5 M $KHCO_3$, pH 7.4	1
	0.056	H_2	0.58			
	0.146	O_2	0.68			
$BiVO_4$ – PVK|GE|Pt	1.26	H_2	10.2	$6.20\cdot10^{-8}$	0.1 M KB_i, 0.1 M K_2SO_4, pH 8.5	31
		O_2	4.95			
$BiVO_4$ – PVK|GE|IO-TiO_2|FDH	0.80	HCOOH (O_2)	7.1	$1.57\cdot10^{-7}$	MOPS, $NaHCO_3$, CsCl, pH 6.4	33
Pt|PVK|$Cu_{30}Pd_{70}$	n.a.	H_2	43.8	$6.32\cdot10^{-6}$	cellulose, 1 M KOH	4
		gluconic acid	26.8			
Pt|PVK|$Cu_{30}Pd_{70}$	n.a.	H_2	70.5	$2.52\cdot10^{-7}$	PET bottle, 1 M KOH	4
		glycolic acid	30.5			
PC sheets						
$RhCrO_x$|CoO_y|$SrTiO_3$:Al	0.4	H_2 (O_2)	4.2	$2.53\cdot10^{-8}$	~ 0.7 Sun (outdoors), H_2O	36
Cr_2O_3|Ru-$SrTiO_3$:La,Rh|Au|$BiVO_4$:Mo	1.1	H_2	19.6	$1.19\cdot10^{-7}$	H_2O, 331 K, 10 kPa	17
		O_2	9.8			
CotpyP-$SrTiO_3$:La,Rh|Au|$BiVO_4$:Mo	0.08	HCOOH	1.09	$3.26\cdot10^{-8}$	0.1 M $KHCO_3$, pH 6.7	2
		H_2	0.03			
		O_2	0.52			
CN_x | Ni_2P panel	n.a.	H_2	0.02	$2.20\cdot10^{-9}$	PET, 0.5 M KOH	3
		HCOOH (mixture)	0.09			
PV panels						
		electricity		$1.09\cdot10^{-6}$	assuming \$0.0685/kWh cost	

Value of chemicals (\$ kg^{-1}), estimated based on NREL procedures[56]: CO_2 - 0.17; CO - 0.44; H_2 - 2.52; O_2 - 0.06; H_2O - $2.9\cdot10^{-4}$; formic acid - 0.63; cellulose - 0.90; PET - 0.27; glycolic acid - 0.63; gluconic acid - 1.99.

5. Reactor engineering and upscaling

5.1. Setup types

Most studies of PEC or PC systems are performed in glassware reactors, which restrict the sample size below 1 cm^2. In contrast, scalability studies require custom-made reactors, which can be fabricated through machining from a solid block of material,[3] from transparent commercial panels,[57,58] or by modern fabrication techniques such as 3D printing (Figure 3).[29,59] Reactors machined from polyether ether ketone (PEEK) are more suitable for waste photoreforming studies, as PEEK can withstand the strongly basic solution (pH ≈ 14) employed under operation.[3] On the other hand, 3D printing offers the unique possibility of fast, inexpensive prototyping, as modular reactors can be printed from polylactic acid (PLA) overnight and assembled the next day. These versatile 3D-printed reactors can be easily adapted to accommodate PEC leaves,[29] PC sheets[2] or individual photoelectrodes of various sizes,[29,51] in two- or three-electrode configurations.

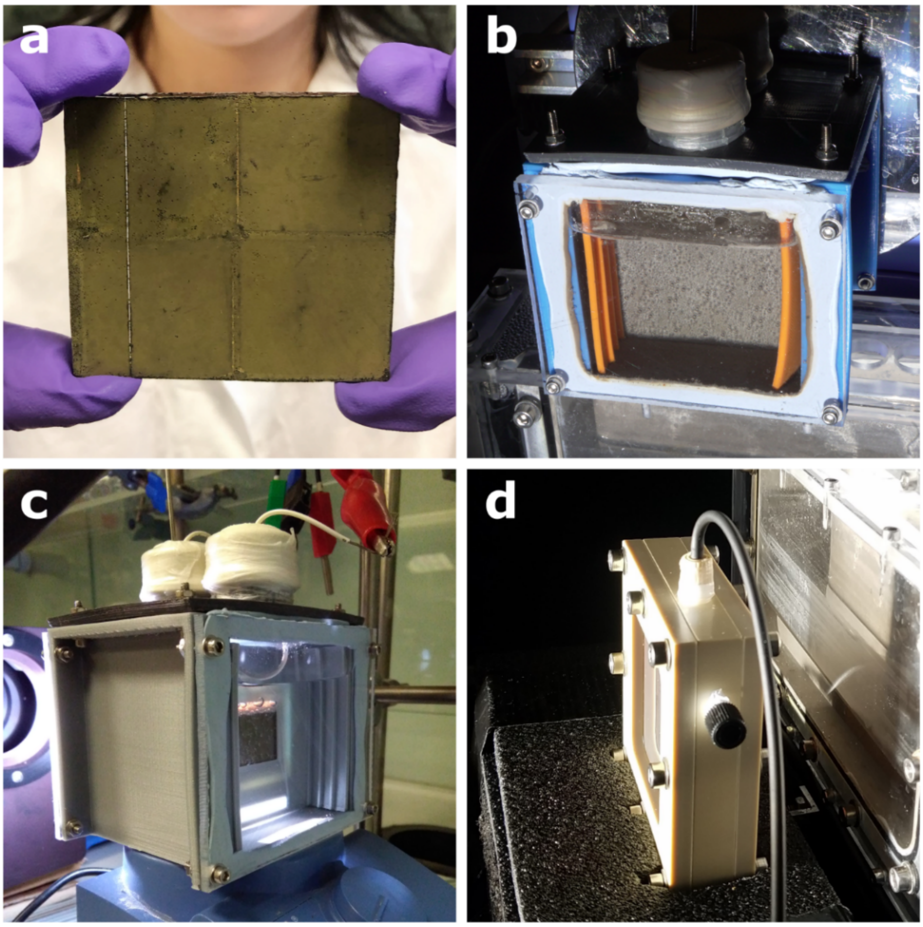

Figure 3. Upscaling. (a) image of a 5×5 cm^2 PC sheet. (b) same PC sheet under operation in a 3D-printed reactor. (c) 2×2 cm^2 PEC leaf in the 3D-printed reactor. (d) PC sheet in a machined flow reactor for photoreforming (5×5 cm^2 window). Adapted with permission from ref. [3]. Copyright 2020 Wiley-VCH GmbH. (b,c) batch reactors, (d) flow reactor.

Reactors can be further categorized into batch or flow systems. Similar considerations apply for batch and flow reactors using panels, as for those using photocatalyst suspensions.[60,61] However, since the light absorber is immobilized, care must be taken in regard to the panel irradiation (direct or through liquid), solution turbidity and reactor geometry. Batch reactors are completely closed; a set quantity of reactants and the resulting products are contained within a set volume for a given timeframe. In flow reactors, the reactant(s) are circulated over an immobilized photocatalyst and the products are collected in a separate vessel. While batch reactors are typically easier to design and construct, they face practical challenges upon scaling, including mass transfer limitations due to stirring inconsistencies across the reactor area and over-pressure development due to gaseous product generation. In contrast, flow reactors maintain constant mixing for improved mass transfer and can provide facile separation and in-line quantification of products and reactants.[62] For slow reactions such as photoreforming, it is crucial to carefully adjust the flow rate to allow for maximal retention time while maintaining sufficient mass transfer.

Typically, oxidative and reductive gaseous products are obtained on different sides of the panel for artificial leaves, which facilitates their separation. In contrast, O_2 and H_2 are produced in close proximity during water splitting, on the same side of PC sheets. Due to the wide flammability range of H_2 (4-94% at ambient temperature and pressure), the safe separation of H_2 from gaseous mixtures requires careful consideration. Using a commercial polyimide membrane, 73% of H_2 was safely separated and recycled from the moist gas mixture produced by overall water splitting over 100 m^2 photocatalyst sheets.[38] However, more than 20% of H_2 remained in the feed gas. Gas separation membranes with a higher H_2 permeability and lower O_2 permeability will be required for operation in the future. These issues can be avoided through photoreforming, as the organic substrates can be selectively oxidized to aqueous products. Hence, H_2 accumulates in the head space, while oxidative products remain dissolved in solution.

In terms of irradiation, laboratory setups often employ a broadband Xe or Hg light source, which is fitted with an AM 1.5G filter to match the output light to the solar spectrum (especially in the UV region). UV-filters (e.g. >420 nm) can be further attached to avoid the degradation of sensitive molecular catalysts, whereas IR water filters mitigate reactor heating. Neutral density filters of varying opacity can also be used to simulate seasonal changes in sunlight intensity, regions with lower solar irradiance, or overcast weather conditions.[1] However, calibrated commercial setups only provide irradiation sizes below 30×30 cm^2, which limits the number and scope of scalability studies. In contrast, low cost light-emitting diode (LED) light sources are well established in organic flow photochemistry and the pharmaceutical industry.[63,64] Such LED arrays provide control over the excitation wavelength, require a low power input and are suitable for indoor use, which made them recently attractive for organic transformations using PC suspensions.[64]

5.2. Practical advantages

From a sustainability perspective, thin film technologies are a crucial step towards reducing the environmental impacts of light-to-chemical conversion. These panel designs offer several general advantages towards solar fuel production. In comparison to PV-EC systems, artificial leaves require no additional wiring, electronics or membranes, which decreases the overall complexity of the system. [12] Such PEC or PC panels are often based on earth abundant elements and operate in benign, (near) neutral pH solutions, which can further decrease their cost of operation.

The energy use and greenhouse gas emissions of the additional materials and processing steps required to fabricate a PC sheet or artificial leaf are approximately 0.234-1.788 $\mathrm{MJ\ m^{-2}_{panel}}$ and 0.016-0.101 $\mathrm{kg_{CO2}\ m^{-2}_{panel}}$, respectively, depending on annealing temperature. These values include the environmental impacts associated with glass substrate production (assumed to be 2 mm thick) and annealing of the PC sheet or artificial leaf at temperatures of 80-450°C (assumed to use an electric furnace); binders such as Nafion were neglected as they comprise a minimal portion of the overall material mass. Given that separating a photocatalyst by centrifugation or vacuum filtration would use 0.072 $\mathrm{MJ\ m^{-2}_{irr}}$ and emit 0.004 $\mathrm{kg_{CO2}\ m^{-2}_{irr}}$ (assuming a 1 cm reactor depth and two separation steps with energy requirements of 1 kWh $\mathrm{m^{-3}_{solution}}$ each),[65] the impacts from immobilization would be negated after 3 to 25 reuse cycles. Separation by vacuum filtration has higher requirements of 0.306 $\mathrm{MJ\ m^{-2}_{irr}}$ and 0.017 $\mathrm{kg_{CO2}\ m^{-2}_{irr}}$ (assuming a filter area of 100 $\mathrm{cm^2}$ and energy use of 8.5 kWh $\mathrm{m^{-2}}$)[66] a PC sheet or artificial leaf could therefore be environmentally beneficial after as little as one reuse cycle.

Catalyst recyclability is therefore a key benefit of immobilization, as thin films can be easily retrieved from the reaction medium compared to homogeneous PC suspensions. For example, the compact $\mathrm{Cu_{30}Pd_{70}}$|perovskite|Pt PEC artificial leaves have shown promising reusability over 4 cycles of PET waste reforming.[4] $\mathrm{CN_x|Ni_2P}$ sheets have been similarly shown to retain over 70% of their $\mathrm{H_2}$ evolution activity after 4 reuse cycles of photoreforming under mildly alkaline conditions (0.5 M KOH), with minimal co-catalyst (0.3% Ni) and photocatalyst (0% $\mathrm{CN_x}$) leaching.[3] This is a marked improvement over a particulate $\mathrm{CN_x|Ni_2P}$ system, which lost half of its efficiency after a single reuse cycle.[21] For photoreforming systems in particular, immobilization also enables the use of turbid waste streams that would otherwise prevent light from reaching a PC suspension. In this case, the transparent glass substrate of PC sheets and wired PEC systems can directly face the light source, acting as a window for the reactor.[3,4]

Furthermore, a PC sheet reactor can be designed to easily track the sun so that direct radiation can be captured more effectively during the day.[67] When compared to a fixed panel array, the baseline levelized production cost of a sun-tracking panel reactor integrated with a solar concentrator can be significantly reduced.[68] The resulting elevated temperatures caused by the photo-thermal effect are also known to improve catalysis.[69–71] Given the similar construction and implementation requirements for thin film solar fuel technologies and photovoltaics, artificial leaves and PC sheets are expected to benefit from expertise in the solar industry, resulting in more facile up-scaling than particulate systems.

5.3. Remaining challenges

Despite their advantages, solar fuel panels suffer from similar scalability challenges to other light harvesting technologies,[72] which result in a non-linear scaling of the performance with the photoactive area (Table 2). One known drawback of artificial leaves is the build-up of a pH difference between the anodic and cathodic sides, which leads to an increase in the overpotential during operation and may affect the catalysis. This effect is particularly detrimental for large-scale devices operating under neutral pH solutions without solution convection.[73] This can be avoided by utilizing electrolyte solutions with either a very low, or high pH (as in the case of PEC waste reforming). Neutral pH solutions can also be employed using controlled convection streams (i.e., solution recirculation), whereas carefully positioned separators can mitigate product crossover.[74,75] Alternatively, the product separation can be attained in microfluidic flow reactors, where closely positioned channels are separated by appropriate ion exchange membranes.[76] On the other hand, resistive losses can occur through a conductive electrode substrate. For example, FTO glass limits the photocurrent of both perovskite photocathodes[29] and $BiVO_4$ photoanodes[51] to below 100 mA. This can be avoided through a monolithic design, where the charge flow only occurs perpendicular to the panel surface (cross-plane).[15]

Table 2. Comparison between the advantages and disadvantages of solar panel technologies.

	Water splitting & CO_2 reduction		**Photoreforming**	
	PEC leaf	PC sheet	PEC leaf	PC sheet
Overall benefits	compact, standalone, facile retrieval and reuse, cost, off-grid applications			
Overall challenges	(catalyst) optimization, translation to real-world applications, product collection			
Light absorbers	tandem		single	
Fabrication	complex	moderate	complex	simple
Areal activity	high	moderate	very high	low
Scalability	moderate	high	moderate	high
Selectivity	high	high	high	moderate
Stability	moderate	high / cocatalyst leaching	moderate	high
Product separation	red. & ox. separated	same side	red. & ox. separated	same side
Impurities & turbidity	side reactions, optical losses	compatible	optical losses	compatible

Both issues can be in principle circumvented by employing the PC sheet design, as charges only travel a small distance between adjacent particles.[17] Consequently, a comparable solar-to-formate conversion efficiency was observed even if the active area was increased 20 times.[2] However, a performance decrease is still sometimes observed for these systems,[3,17] which can be linked to manufacturing inhomogeneity and mass transport limitations on a large scale. A careful optimization of (photo)catalytic deposition procedures and reactor design will therefore be necessary to minimize material inconsistencies, promote mass transport, and balance trade-offs between light absorption and charge recombination.

Besides fabrication, product separation and scalability, current panel technologies can suffer from light absorber or catalyst degradation, which manifests through moisture infiltration or catalyst leaching. This limits the stability of state-of-the-art systems to several weeks, whereas oxide-based compounds have been shown to operate for over several months under real-world conditions.[38] Despite the interplay between stability and performance, we recently demonstrated that artificial leaves can also perform overall water splitting over several hundred hours, by employing an oxide-based device structure and suitable hydrophobic encapsulation.[77]

Recent technoeconomic analysis has also suggested that PC sheets could be slightly more expensive than particulate systems (by ~12%) due to increased reactor complexity and corresponding cost.[78] However, these results are dependent on the assumed PC recyclability in the different systems. Our own technoeconomic analysis of (slurry) waste photoreforming showed that higher photocatalyst lifetimes of 1-10 years, which may be more feasible with a robust thin film system, can significantly reduce both cost and environmental impacts.[40]

6. Broader reaction scope and applications

The thin film solar panel technologies discussed in this Account can in principle be utilized for applications beyond solar fuels. Photoreforming with PEC leaf or PC sheet systems already addresses the waste management sector, as it is capable of converting a diverse range of biomass, plastics and industrial by-products into organic chemicals. This reaction scope could be further expanded to other problematic waste streams containing pollutants,[79] agricultural or medical waste, and especially opaque materials that prevent effective photoreforming under slurry conditions. It should nevertheless be noted that chemical, thermal, or biological pre-treatments will likely be required to release soluble substrates that can easily diffuse to the thin film surface and undergo oxidation.

Moreover, both PC and PEC approaches may be employed in the synthesis of higher value chemicals. While organic transformations are often performed in PC flow systems,[63] the potential of photoelectrodes (for instance Fe_2O_3) towards synthesis has only been recognized recently.[80] PEC systems in particular can offer controlled oxidation through the use of certain applied potentials or selective co-catalysts. This capability not only ensures a selective product stream that can have commercial value, but also prevents over-oxidation of substrates to undesirable CO_2.[4] We have already demonstrated the production of value-added organic products (glycolic acid, glyceric acid, formic acid, among others).[4] The synthesis of cyclobutanes – building blocks for some pharmaceutical compounds – over immobilized CN_x has also been recently reported.[81] With sufficient catalyst design, integrated panels could be applied to the production of fine chemicals or pharmaceuticals, helping to decarbonize industries that are currently reliant on fossil fuels for both feedstocks and reaction conditions (i.e., heat, pressure).

7. Conclusions and outlook

Despite their differences in naming, assembly and operating principle, thin film solar panel technologies share a common design, which makes them stand out among light harvesting technologies. Such panels have recently demonstrated their versatility for a wide range of reactions beyond water splitting, including CO_2 reduction and organic transformations. For the latter, the lower thermodynamic threshold required to oxidize organics provides an advantage, which can enable those systems to match the production rates of conventional PV-EC systems. The integration of all components in standalone PEC artificial leaves results in a material cost reduction. Furthermore, the recyclability of such panels can offset the cost and environmental impacts associated with PC particle immobilization.

While these systems are yet mostly developed on a lab scale, further improvements in terms of scalability, stability and performance could make them attractive from an economic perspective. Here, the modularity of the systems can provide a key advantage, as solar fuels panels would benefit from progress in the established electrocatalysis and photovoltaics communities.[77] Once such systems can sustain competitive product rates over several years on a square-meter scale, they could be deployed for commercial applications. In a conservative scenario, solar panels may find use in the fine chemical synthesis, where the value of the products outweighs the lower product rates compared to water and CO_2 electrolysis. In the long term, such panels would ideally contribute to a circular fuel and chemicals economy, thereby closing the carbon cycle.

Acknowledgements

This work was supported by St. John' College Cambridge (Title A Fellowship), an EU Marie Sklodowska-Curie individual Fellowship (GAN 793996), the EPSRC Cambridge NanoDTC (EP/L015978/1 and EP/S022953/1), a HRH The Prince of Wales Commonwealth Scholarship and a European Research Council Consolidator Grant "MatEnSAP" (No. 682833) and Proof of Concept Grant "SolReGen" (No. 966581).

Biographical Information

Virgil Andrei obtained his Bachelor and Master of Science degrees in chemistry from Humboldt-Universität zu Berlin, where he studied thermoelectric polymer pastes and films in the group of Prof. Klaus Rademann (2014-2016). He then pursued a PhD in chemistry at the University of Cambridge (2016-2020), where he developed perovskite-based artificial leaves in the group of Prof. Erwin Reisner, working closely with the Optoelectronics group of Prof. Richard Friend at the Cavendish Laboratory. He is currently a Title A Research Fellow at St John's College, Cambridge, and a visiting Winton fellow in the group of Prof. Peidong Yang at University of California, Berkeley. His work places a strong focus on scalability, material design, complementary light harvesting and synthesis of added-value carbon products, introducing modern fabrication techniques towards low-cost, high-throughput solar fuel production.

Qian Wang received her Ph.D. in 2014 at the University of Tokyo, Japan, where she worked on the development of perovskite-type oxide photocatalysts for visible-light-driven water splitting under the guidance of Prof. Kazunari Domen. She then worked as a postdoctoral researcher at the Japan Technological Research Association of Artificial Photosynthetic Chemical Processes (ARPChem) on the development of standalone photocatalyst devices for overall water splitting. In 2018, she became a

Marie Sklodowska-Curie Research Fellow to develop inorganic-organic hybrid photocatalyst sheets for CO_2 reduction at Prof. Erwin Reisner's group at the University of Cambridge. She joined Nagoya University as an Associate Professor in May 2021 and established her research group, which is currently developing new materials, approaches, and technologies for solar energy storage in the form of renewable fuels via artificial photosynthesis.

Taylor Uekert received her bachelor's degree in NanoEngineering from the University of California San Diego (2016), followed by a master's degree in Nanoscience & Nanotechnology and a PhD in Chemistry from the University of Cambridge (2017, 2021). For her PhD research, she studied photoreforming of plastic and mixed waste to hydrogen fuel and organic chemicals using semiconductor suspensions and panels under the guidance of Prof. Erwin Reisner. She is currently an analyst at the National Renewable Energy Laboratory, where her research interests include circular economy strategies for renewable energy technologies, plastic, and food.

Subhajit Bhattacharjee received his integrated Bachelor's and Master's (BS-MS) degree in Chemical Sciences from the Indian Institute of Science Education and Research (IISER) Kolkata in 2019. He is currently pursuing his Ph.D. under the guidance of Prof. Erwin Reisner at the University of Cambridge, UK. His research broadly lies in the domain of materials and energy sciences, and primarily focuses on the design, development and engineering of PEC cells and artificial leaves for sustainable energy production, waste valorization and CO_2 utilization.

Erwin Reisner received his education and professional training at the University of Vienna (PhD in 2005), the Massachusetts Institute of Technology (postdoc from 2005-2007) and the University of Oxford (postdoc from 2008-2009). He joined the University of Cambridge as a University Lecturer in the Department of Chemistry in 2010, became a Fellow of St. John's College in 2011, was appointed to Reader in 2015 and to his current position of Professor of Energy and Sustainability in 2017. His laboratory develops solar-powered valorisation technologies for the conversion of water, carbon dioxide and solid waste streams such as biomass and plastics to fuels and chemicals for a circular economy.

References

(1) Andrei, V.; Reuillard, B.; Reisner, E. Bias-free solar syngas production by integrating a molecular cobalt catalyst with perovskite–$BiVO_4$ tandems. *Nat. Mater.* **2020**, *19*, 189–194. DOI: 10.1038/s41563-019-0501-6.
(2) Wang, Q.; Warnan, J.; Rodríguez-Jiménez, S.; Leung, J. J.; Kalathil, S.; Andrei, V.; Domen, K.; Reisner, E. Molecularly engineered photocatalyst sheet for scalable solar formate production from carbon dioxide and water. *Nat. Energy* **2020**, *5* (9), 703–710. DOI: 10.1038/s41560-020-0678-6.
(3) Uekert, T.; Bajada, M. A.; Schubert, T.; Pichler, C. M.; Reisner, E. Scalable Photocatalyst Panels for Photoreforming of Plastic, Biomass and Mixed Waste in Flow. *ChemSusChem* **2021**, *14* (19), 4190–4197. DOI: 10.1002/cssc.202002580.
(4) Bhattacharjee, S.; Andrei, V.; Pornrungroj, C.; Rahaman, M.; Pichler, C. M.; Reisner, E. Reforming of Soluble Biomass and Plastic Derived Waste Using a Bias-

Free $Cu_{30}Pd_{70}$|Perovskite|Pt Photoelectrochemical Device. *Adv. Funct. Mater.* **2022**, *32* (7), 2109313. DOI: 10.1002/adfm.202109313.

(5) Fujishima, A.; Honda, K. Electrochemical Photolysis of Water at a Semiconductor Electrode. *Nature* **1972**, *238* (5358), 37–38. DOI: 10.1038/238037a0.

(6) McKone, J. R.; Lewis, N. S.; Gray, H. B. Will Solar-Driven Water-Splitting Devices See the Light of Day? *Chem. Mater.* **2014**, *26* (1), 407–414. DOI: 10.1021/cm4021518.

(7) Wang, Q.; Domen, K. Particulate Photocatalysts for Light-Driven Water Splitting: Mechanisms, Challenges, and Design Strategies. *Chem. Rev.* **2020**, *120* (2), 919–985. DOI: 10.1021/acs.chemrev.9b00201.

(8) Kim, J. H.; Hansora, D.; Sharma, P.; Jang, J.-W.; Lee, J. S. Toward practical solar hydrogen production – an artificial photosynthetic leaf-to-farm challenge. *Chem. Soc. Rev.* **2019**, *48* (7), 1908–1971. DOI: 10.1039/C8CS00699G.

(9) Licht, S.; Wang, B.; Mukerji, S.; Soga, T.; Umeno, M.; Tributsch, H. Efficient Solar Water Splitting, Exemplified by RuO_2-Catalyzed AlGaAs/Si Photoelectrolysis. *J. Phys. Chem. B* **2000**, *104* (38), 8920–8924. DOI: 10.1021/jp002083b.

(10) Su, Y.; Cestellos-Blanco, S.; Kim, J. M.; Shen, Y.-x.; Kong, Q.; Lu, D.; Liu, C.; Zhang, H.; Cao, Y.; Yang, P. Close-Packed Nanowire-Bacteria Hybrids for Efficient Solar-Driven CO_2 Fixation. *Joule* **2020**, *4* (4), 800–811. DOI: 10.1016/j.joule.2020.03.001.

(11) Dogutan, D. K.; Nocera, D. G. Artificial Photosynthesis at Efficiencies Greatly Exceeding That of Natural Photosynthesis. *Acc. Chem. Res.* **2019**, *52* (11), 3143–3148. DOI: 10.1021/acs.accounts.9b00380.

(12) Joya, K. S.; Joya, Y. F.; Ocakoglu, K.; van de Krol, Roel. Water-Splitting Catalysis and Solar Fuel Devices: Artificial Leaves on the Move. *Angew. Chem. Int. Ed.* **2013**, *52* (40), 10426–10437. DOI: 10.1002/anie.201300136.

(13) Kato, H.; Hori, M.; Konta, R.; Shimodaira, Y.; Kudo, A. Construction of Z-scheme Type Heterogeneous Photocatalysis Systems for Water Splitting into H_2 and O_2 under Visible Light Irradiation. *Chem. Lett.* **2004**, *33* (10), 1348–1349. DOI: 10.1246/cl.2004.1348.

(14) Sasaki, Y.; Iwase, A.; Kato, H.; Kudo, A. The effect of co-catalyst for Z-scheme photocatalysis systems with an Fe^{3+}/Fe^{2+} electron mediator on overall water splitting under visible light irradiation. *J. Catal.* **2008**, *259* (1), 133–137. DOI: 10.1016/j.jcat.2008.07.017.

(15) Reece, S. Y.; Hamel, J. A.; Sung, K.; Jarvi, T. D.; Esswein, A. J.; Pijpers, Joep J. H.; Nocera, D. G. Wireless Solar Water Splitting Using Silicon-Based Semiconductors and Earth-Abundant Catalysts. *Science* **2011**, *334* (6056), 645–648. DOI: 10.1126/science.1209816.

(16) Nocera, D. G. The Artificial Leaf. *Acc. Chem. Res.* **2012**, *45* (5), 767–776. DOI: 10.1021/ar2003013.

(17) Wang, Q.; Hisatomi, T.; Jia, Q.; Tokudome, H.; Zhong, M.; Wang, C.; Pan, Z.; Takata, T.; Nakabayashi, M.; Shibata, N.; Li, Y.; Sharp, I. D.; Kudo, A.; Yamada, T.; Domen, K. Scalable water splitting on particulate photocatalyst sheets with a solar-to-hydrogen energy conversion efficiency exceeding 1%. *Nat. Mater.* **2016**, *15*, 611.

(18) Wang, Q.; Hisatomi, T.; Suzuki, Y.; Pan, Z.; Seo, J.; Katayama, M.; Minegishi, T.; Nishiyama, H.; Takata, T.; Seki, K.; Kudo, A.; Yamada, T.; Domen, K. Particulate Photocatalyst Sheets Based on Carbon Conductor Layer for Efficient Z-Scheme Pure-Water Splitting at Ambient Pressure. *J. Am. Chem. Soc.* **2017**, *139* (4), 1675–1683. DOI: 10.1021/jacs.6b12164.

(19) Kasap, H.; Achilleos, D. S.; Huang, A.; Reisner, E. Photoreforming of Lignocellulose into H_2 Using Nanoengineered Carbon Nitride under Benign Conditions. *J. Am. Chem. Soc.* **2018**, *140* (37), 11604–11607. DOI: 10.1021/jacs.8b07853.

(20) Achilleos, D. S.; Yang, W.; Kasap, H.; Savateev, A.; Markushyna, Y.; Durrant, J. R.; Reisner, E. Solar Reforming of Biomass with Homogeneous Carbon Dots. *Angew. Chem. Int. Ed.* **2020**, *59* (41), 18184–18188. DOI: 10.1002/anie.202008217.

(21) Uekert, T.; Kasap, H.; Reisner, E. Photoreforming of Nonrecyclable Plastic Waste over a Carbon Nitride/Nickel Phosphide Catalyst. *J. Am. Chem. Soc.* **2019**, *141* (38), 15201–15210. DOI: 10.1021/jacs.9b06872.

(22) Nielander, A. C.; Shaner, M. R.; Papadantonakis, K. M.; Francis, S. A.; Lewis, N. S. A taxonomy for solar fuels generators. *Energy Environ. Sci.* **2015**, *8* (1), 16–25. DOI: 10.1039/C4EE02251C.

(23) Holmes-Gentle, I.; Haussener, S.; van de Krol, Roel; Hankin, A.; Page, H.; Abdi, F.; Ahmet, I.; Bedoya-Lora, F.; David, F. *SolarFuelsDB*. https://www.solarfuelsdb.epfl.ch/ (accessed 2022-02-26).

(24) Nguyen, D. N.; Fadel, M.; Chenevier, P.; Artero, V.; Tran, P. D. Water-Splitting Artificial Leaf Based on a Triple-Junction Silicon Solar Cell: One-Step Fabrication through Photoinduced Deposition of Catalysts and Electrochemical Operando Monitoring. *J. Am. Chem. Soc.* **2022.** DOI: 10.1021/jacs.2c00666.

(25) Kim, J. H.; Jo, Y.; Kim, J. H.; Jang, J. W.; Kang, H. J.; Lee, Y. H.; Kim, D. S.; Jun, Y.; Lee, J. S. Wireless Solar Water Splitting Device with Robust Cobalt-Catalyzed, Dual-Doped $BiVO_4$ Photoanode and Perovskite Solar Cell in Tandem: A Dual Absorber Artificial Leaf. *ACS Nano* **2015**, *9* (12), 11820–11829. DOI: 10.1021/acsnano.5b03859.

(26) Yang, W.; Prabhakar, R. R.; Tan, J.; Tilley, S. D.; Moon, J. Strategies for enhancing the photocurrent, photovoltage, and stability of photoelectrodes for photoelectrochemical water splitting. *Chem. Soc. Rev.* **2019**, *48* (19), 4979–5015. DOI: 10.1039/C8CS00997J.

(27) Arai, T.; Sato, S.; Kajino, T.; Morikawa, T. Solar CO_2 reduction using H_2O by a semiconductor/metal-complex hybrid photocatalyst: enhanced efficiency and demonstration of a wireless system using $SrTiO_3$ photoanodes. *Energy Environ. Sci.* **2013**, *6* (4), 1274–1282. DOI: 10.1039/C3EE24317F.

(28) Arai, T.; Sato, S.; Morikawa, T. A monolithic device for CO_2 photoreduction to generate liquid organic substances in a single-compartment reactor. *Energy Environ. Sci.* **2015**, *8* (7), 1998–2002. DOI: 10.1039/C5EE01314C.

(29) Andrei, V.; Hoye, R. L. Z.; Crespo-Quesada, M.; Bajada, M.; Ahmad, S.; Volder, M. de; Friend, R.; Reisner, E. Scalable Triple Cation Mixed Halide Perovskite–$BiVO_4$ Tandems for Bias-Free Water Splitting. *Adv. Energy Mater.* **2018**, *8*, 1801403. DOI: 10.1002/aenm.201801403.

(30) Rahaman, M.; Andrei, V.; Pornrungroj, C.; Wright, D.; Baumberg, J. J.; Reisner, E. Selective CO production from aqueous CO_2 using a $Cu_{96}In_4$ catalyst and its integration into a bias-free solar perovskite–$BiVO_4$ tandem device. *Energy Environ. Sci.* **2020**, *13* (10), 3536–3543. DOI: 10.1039/D0EE01279C.

(31) Pornrungroj, C.; Andrei, V.; Rahaman, M.; Uswachoke, C.; Joyce, H. J.; Wright, D. S.; Reisner, E. Bifunctional Perovskite-$BiVO_4$ Tandem Devices for Uninterrupted Solar and Electrocatalytic Water Splitting Cycles. *Adv. Funct. Mater.* **2021**, *31* (15), 2008182. DOI: 10.1002/adfm.202008182.

(32) Andrei, V.; Ucoski, G. M.; Pornrungroj, C.; Uswachoke, C.; Wang, Q.; Achilleos, D. S.; Kasap, H.; Sokol, K. P.; Jagt, R. A.; Lu, H.; Lawson, T.; Wagner, A.; Pike, S.

D.; Wright, D. S.; Hoye, R. L. Z.; MacManus-Driscoll, J. L.; Joyce, H. J.; Friend, R. H.; Reisner, E. Floating perovskite-$BiVO_4$ devices for scalable solar fuel production. *Nature* **2022**, *608* (7923), 518–522. DOI: 10.1038/s41586-022-04978-6.

(33) Edwardes Moore, E.; Andrei, V.; Oliveira, A. R.; Coito, A. M.; Pereira, I. A. C.; Reisner, E. A Semi-artificial Photoelectrochemical Tandem Leaf with a CO_2-to-Formate Efficiency Approaching 1 %. *Angew. Chem. Int. Ed.* **2021**, *60* (50), 26303–26307. DOI: 10.1002/anie.202110867.

(34) Edwardes Moore, E.; Andrei, V.; Zacarias, S.; Pereira, I. A. C.; Reisner, E. Integration of a Hydrogenase in a Lead Halide Perovskite Photoelectrode for Tandem Solar Water Splitting. *ACS Energy Lett.* **2020**, *5* (1), 232–237. DOI: 10.1021/acsenergylett.9b02437.

(35) Sokol, K. P.; Robinson, W. E.; Warnan, J.; Kornienko, N.; Nowaczyk, M. M.; Ruff, A.; Zhang, J. Z.; Reisner, E. Bias-free photoelectrochemical water splitting with photosystem II on a dye-sensitized photoanode wired to hydrogenase. *Nat. Energy* **2018**, *3* (11), 944–951. DOI: 10.1038/s41560-018-0232-y.

(36) Goto, Y.; Hisatomi, T.; Wang, Q.; Higashi, T.; Ishikiriyama, K.; Maeda, T.; Sakata, Y.; Okunaka, S.; Tokudome, H.; Katayama, M.; Akiyama, S.; Nishiyama, H.; Inoue, Y.; Takewaki, T.; Setoyama, T.; Minegishi, T.; Takata, T.; Yamada, T.; Domen, K. A Particulate Photocatalyst Water-Splitting Panel for Large-Scale Solar Hydrogen Generation. *Joule* **2018**, *2* (3), 509–520. DOI: 10.1016/j.joule.2017.12.009.

(37) Xiong, A.; Ma, G.; Maeda, K.; Takata, T.; Hisatomi, T.; Setoyama, T.; Kubota, J.; Domen, K. Fabrication of photocatalyst panels and the factors determining their activity for water splitting. *Catal. Sci. Technol.* **2014**, *4* (2), 325–328. DOI: 10.1039/C3CY00845B.

(38) Nishiyama, H.; Yamada, T.; Nakabayashi, M.; Maehara, Y.; Yamaguchi, M.; Kuromiya, Y.; Tokudome, H.; Akiyama, S.; Watanabe, T.; Narushima, R.; Okunaka, S.; Shibata, N.; Takata, T.; Hisatomi, T.; Domen, K. Photocatalytic solar hydrogen production from water on a 100 m^2-scale. *Nature* **2021**, *598*, 304–307. DOI: 10.1038/s41586-021-03907-3.

(39) Wang, Q.; Kalathil, S.; Pornrungroj, C.; Sahm, C. D.; Reisner, E. Bacteria–photocatalyst sheet for sustainable carbon capture and utilization. *Nat. Catal.* **2022.** DOI: 10.1038/s41929-022-00817-z.

(40) Uekert, T.; Pichler, C. M.; Schubert, T.; Reisner, E. Solar-driven reforming of solid waste for a sustainable future. *Nat. Sustain.* **2021**, *4* (5), 383–391. DOI: 10.1038/s41893-020-00650-x.

(41) Zhang, Y.; Tang, B.; Wu, Z.; Shi, H.; Zhang, Y.; Zhao, G. Glucose oxidation over ultrathin carbon-coated perovskite modified TiO_2 nanotube photonic crystals with high-efficiency electron generation and transfer for photoelectrocatalytic hydrogen production. *Green Chem.* **2016**, *18* (8), 2424–2434. DOI: 10.1039/C5GC02745D.

(42) Esposito, D. V.; Forest, R. V.; Chang, Y.; Gaillard, N.; McCandless, B. E.; Hou, S.; Lee, K. H.; Birkmire, R. W.; Chen, J. G. Photoelectrochemical reforming of glucose for hydrogen production using a WO_3-based tandem cell device. *Energy Environ. Sci.* **2012**, *5* (10), 9091–9099. DOI: 10.1039/C2EE22560C.

(43) Madriz, L.; Tatá, J.; Carvajal, D.; Núñez, O.; Scharifker, B. R.; Mostany, J.; Borrás, C.; Cabrerizo, F. M.; Vargas, R. Photocatalysis and photoelectrochemical glucose oxidation on Bi_2WO_6: Conditions for the concomitant H_2 production. *Renewable Energy* **2020**, *152*, 974–983. DOI: 10.1016/j.renene.2020.01.071.

(44) Huang, L.-W.; Vo, T.-G.; Chiang, C.-Y. Converting glycerol aqueous solution to hydrogen energy and dihydroxyacetone by the $BiVO_4$ photoelectrochemical cell. *Electrochim. Acta* **2019**, *322*, 134725. DOI: 10.1016/j.electacta.2019.134725.

(45) Bashiri, R.; Mohamed, N. M.; Fai Kait, C.; Sufian, S.; Khatani, M. Enhanced hydrogen production over incorporated Cu and Ni into titania photocatalyst in glycerol-based photoelectrochemical cell: Effect of total metal loading and calcination temperature. *Int. J. Hydrogen Energy* **2017**, *42* (15), 9553–9566. DOI: 10.1016/j.ijhydene.2017.01.225.

(46) Ibadurrohman, M.; Hellgardt, K. Photoelectrochemical performance of graphene-modified TiO_2 photoanodes in the presence of glycerol as a hole scavenger. *Int. J. Hydrogen Energy* **2014**, *39* (32), 18204–18215. DOI: 10.1016/j.ijhydene.2014.08.142.

(47) Wang, D.; Lee, S. H.; Han, S.; Kim, J.; Trang, N. V. T.; Kim, K.; Choi, E.-G.; Boonmongkolras, P.; Lee, Y. W.; Shin, B.; Kim, Y. H.; Park, C. B. Lignin-fueled photoelectrochemical platform for light-driven redox biotransformation. *Green Chem.* **2020**, *22* (15), 5151–5160. DOI: 10.1039/D0GC01521K.

(48) Fouad, K.; Bassyouni, M.; Alalm, M. G.; Saleh, M. Y. Recent developments in recalcitrant organic pollutants degradation using immobilized photocatalysts. *Appl. Phys. A* **2021**, *127* (8), 612. DOI: 10.1007/s00339-021-04724-1.

(49) Schröder, M.; Kailasam, K.; Borgmeyer, J.; Neumann, M.; Thomas, A.; Schomäcker, R.; Schwarze, M. Hydrogen Evolution Reaction in a Large-Scale Reactor using a Carbon Nitride Photocatalyst under Natural Sunlight Irradiation. *Energy Technol.* **2015**, *3* (10), 1014–1017. DOI: 10.1002/ente.201500142.

(50) Pichler, C. M.; Bhattacharjee, S.; Rahaman, M.; Uekert, T.; Reisner, E. Conversion of Polyethylene Waste into Gaseous Hydrocarbons via Integrated Tandem Chemical–Photo/Electrocatalytic Processes. *ACS Catal.* **2021**, *11* (15), 9159–9167. DOI: 10.1021/acscatal.1c02133.

(51) Lu, H.; Andrei, V.; Jenkinson, K. J.; Regoutz, A.; Li, N.; Creissen, C. E.; Wheatley, Andrew E. H.; Hao, H.; Reisner, E.; Wright, D. S.; Pike, S. D. Single-Source Bismuth (Transition Metal) Polyoxovanadate Precursors for the Scalable Synthesis of Doped $BiVO_4$ Photoanodes. *Adv. Mater.* **2018**, *30* (46), 1804033. DOI: 10.1002/adma.201804033.

(52) Wang, Q.; Okunaka, S.; Tokudome, H.; Hisatomi, T.; Nakabayashi, M.; Shibata, N.; Yamada, T.; Domen, K. Printable Photocatalyst Sheets Incorporating a Transparent Conductive Mediator for Z-Scheme Water Splitting. *Joule* **2018**, *2* (12), 2667–2680. DOI: 10.1016/j.joule.2018.08.003.

(53) Nitopi, S.; Bertheussen, E.; Scott, S. B.; Liu, X.; Engstfeld, A. K.; Horch, S.; Seger, B.; Stephens, I. E. L.; Chan, K.; Hahn, C.; Nørskov, J. K.; Jaramillo, T. F.; Chorkendorff, I. Progress and Perspectives of Electrochemical CO_2 Reduction on Copper in Aqueous Electrolyte. *Chem. Rev.* **2019**, *119* (12), 7610–7672. DOI: 10.1021/acs.chemrev.8b00705.

(54) Osterloh, F. E. Photocatalysis versus Photosynthesis: A Sensitivity Analysis of Devices for Solar Energy Conversion and Chemical Transformations. *ACS Energy Lett.* **2017**, *2* (2), 445–453. DOI: 10.1021/acsenergylett.6b00665.

(55) Gao, J.; Sahli, F.; Liu, C.; Ren, D.; Guo, X.; Werner, J.; Jeangros, Q.; Zakeeruddin, S. M.; Ballif, C.; Grätzel, M.; Luo, J. Solar Water Splitting with Perovskite/Silicon Tandem Cell and TiC-Supported Pt Nanocluster Electrocatalyst. *Joule* **2019**, *3* (12), 2930–2941. DOI: 10.1016/j.joule.2019.10.002.

(56) Kobos, P. H.; Drennen, T. E.; Outkin, A. V.; Webb, E. K.; Paap, S. M.; Wiryadinata, S. *Techno-Economic Analysis: Best Practices and Assessment Tools*. https://www.osti.gov/biblio/1738878.

(57) Ahmet, I. Y.; Ma, Y.; Jang, J.-W.; Henschel, T.; Stannowski, B.; Lopes, T.; Vilanova, A.; Mendes, A.; Abdi, F. F.; van de Krol, Roel. Demonstration of a 50 cm^2 BiVO4 tandem photoelectrochemical-photovoltaic water splitting device. *Sustainable Energy Fuels* **2019**, *3* (9), 2366-2379. DOI: 10.1039/C9SE00246D.

(58) Kato, N.; Takeda, Y.; Kawai, Y.; Nojiri, N.; Shiozawa, M.; Mizuno, S.; Yamanaka, K.-i.; Morikawa, T.; Hamaguchi, T. Solar Fuel Production from CO_2 Using a 1 m-Square-Sized Reactor with a Solar-to-Formate Conversion Efficiency of 10.5%. *ACS Sustainable Chem. Eng.* **2021**, *9* (48), 16031–16037. DOI: 10.1021/acssuschemeng.1c06390.

(59) Sokol, K. P.; Andrei, V. Automated synthesis and characterization techniques for solar fuel production. *Nat. Rev. Mater.* **2022**, *7*, 251–253. DOI: 10.1038/s41578-022-00432-1.

(60) Ziegenbalg, D.; Pannwitz, A.; Rau, S.; Dietzek-Ivanšić, B.; Streb, C. Comparative Evaluation of Light-Driven Catalysis: A Framework for Standardized Reporting of Data**. *Angewandte Chemie International Edition* **2022**, *61* (28), e202114106. DOI: 10.1002/anie.202114106.

(61) Cambié, D.; Bottecchia, C.; Straathof, N. J. W.; Hessel, V.; Noël, T. Applications of Continuous-Flow Photochemistry in Organic Synthesis, Material Science, and Water Treatment. *Chemical Reviews* **2016**, *116* (17), 10276–10341. DOI: 10.1021/acs.chemrev.5b00707.

(62) Plutschack, M. B.; Pieber, B.; Gilmore, K.; Seeberger, P. H. The Hitchhiker’s Guide to Flow Chemistry. *Chem. Rev.* **2017**, *117* (18), 11796–11893. DOI: 10.1021/acs.chemrev.7b00183.

(63) Buglioni, L.; Raymenants, F.; Slattery, A.; Zondag, S. D. A.; Noël, T. Technological Innovations in Photochemistry for Organic Synthesis: Flow Chemistry, High-Throughput Experimentation, Scale-up, and Photoelectrochemistry. *Chem. Rev.* **2022**, *122* (2), 2752–2906. DOI: 10.1021/acs.chemrev.1c00332.

(64) Ghosh, I.; Khamrai, J.; Savateev, A.; Shlapakov, N.; Antonietti, M.; König, B. Organic semiconductor photocatalyst can bifunctionalize arenes and heteroarenes. *Science* **2019**, *365* (6451), 360–366. DOI: 10.1126/science.aaw3254.

(65) Szepessy, S.; Thorwid, P. Low Energy Consumption of High-Speed Centrifuges. *Chem. Eng. Technol.* **2018**, *41* (12), 2375–2384. DOI: 10.1002/ceat.201800292.

(66) Huttunen, M.; Nygren, L.; Kinnarinen, T.; Häkkinen, A.; Lindh, T.; Ahola, J.; Karvonen, V. Specific energy consumption of cake dewatering with vacuum filters. *Minerals Engineering* **2017**, *100*, 144–154. DOI: 10.1016/j.mineng.2016.10.025.

(67) Pinaud, B. A.; Benck, J. D.; Seitz, L. C.; Forman, A. J.; Chen, Z.; Deutsch, T. G.; James, B. D.; Baum, K. N.; Baum, G. N.; Ardo, S.; Wang, H.; Miller, E.; Jaramillo, T. F. Technical and economic feasibility of centralized facilities for solar hydrogen production via photocatalysis and photoelectrochemistry. *Energy Environ. Sci.* **2013**, *6* (7), 1983–2002. DOI: 10.1039/C3EE40831K.

(68) Wang, Q.; Pornrungroj, C.; Linley, S.; Reisner, E. Strategies to improve light utilization in solar fuel synthesis. *Nat. Energy* **2022**, *7* (1), 13–24. DOI: 10.1038/s41560-021-00919-1.

(69) Mateo, D.; Cerrillo, J. L.; Durini, S.; Gascon, J. Fundamentals and applications of photo-thermal catalysis. *Chem. Soc. Rev.* **2021**, *50* (3), 2173–2210. DOI: 10.1039/D0CS00357C.

(70) Han, B.; Hu, Y. H. Highly Efficient Temperature-Induced Visible Light Photocatalytic Hydrogen Production from Water. *The Journal of Physical Chemistry C* **2015**, *119* (33), 18927–18934. DOI: 10.1021/acs.jpcc.5b04894.
(71) Fang, S.; Hu, Y. H. Thermo-photo catalysis: a whole greater than the sum of its parts. *Chem. Soc. Rev.* **2022**, *51* (9), 3609–3647. DOI: 10.1039/D1CS00782C.
(72) Li, Z.; Klein, T. R.; Kim, D. H.; Yang, M.; Berry, J. J.; van Hest, Maikel F. A. M.; Zhu, K. Scalable fabrication of perovskite solar cells. *Nat. Rev. Mater.* **2018**, *3* (4), 18017. DOI: 10.1038/natrevmats.2018.17.
(73) Singh, M. R.; Xiang, C.; Lewis, N. S. Evaluation of flow schemes for near-neutral pH electrolytes in solar-fuel generators. *Sustainable Energy Fuels* **2017**, *1* (3), 458–466. DOI: 10.1039/C7SE00062F.
(74) Haussener, S.; Xiang, C.; Spurgeon, J. M.; Ardo, S.; Lewis, N. S.; Weber, A. Z. Modeling, simulation, and design criteria for photoelectrochemical water-splitting systems. *Energy Environ. Sci.* **2012**, *5* (12), 9922–9935. DOI: 10.1039/C2EE23187E.
(75) Modestino, M. A.; Walczak, K. A.; Berger, A.; Evans, C. M.; Haussener, S.; Koval, C.; Newman, J. S.; Ager, J. W.; Segalman, R. A. Robust production of purified H_2 in a stable, self-regulating, and continuously operating solar fuel generator. *Energy Environ. Sci.* **2014**, *7* (1), 297–301. DOI: 10.1039/C3EE43214A.
(76) Modestino, M. A.; Diaz-Botia, C. A.; Haussener, S.; Gomez-Sjoberg, R.; Ager, J. W.; Segalman, R. A. Integrated microfluidic test-bed for energy conversion devices. *Phys. Chem. Chem. Phys.* **2013**, *15* (19), 7050–7054. DOI: 10.1039/C3CP51302E.
(77) Andrei, V.; Jagt, R. A.; Rahaman, M.; Lari, L.; Lazarov, V. K.; MacManus-Driscoll, J. L.; Hoye, R. L. Z.; Reisner, E. Long-term solar water and CO_2 splitting with photoelectrochemical BiOI–$BiVO_4$ tandems. *Nat. Mater.* **2022**, *21*, 864–868. DOI: 10.1038/s41563-022-01262-w.
(78) Toe, C. Y.; Pan, J.; Scott, J.; Amal, R. Identifying Key Design Criteria for Large-Scale Photocatalytic Hydrogen Generation from Engineering and Economic Perspectives. *ACS ES&T Engg.* **2022.** DOI: 10.1021/acsestengg.2c00030.
(79) Achilleos, D.; Kasap, H.; Reisner, E. Photocatalytic Hydrogen Generation Coupled to Pollutant Utilization Using Carbon Dots Produced from Biomass. *Green Chem.* **2020**, *22*, 2831-2839. DOI: 10.1039/D0GC00318B.
(80) Zhang, L.; Liardet, L.; Luo, J.; Ren, D.; Grätzel, M.; Hu, X. Photoelectrocatalytic arene C–H amination. *Nat. Catal.* **2019**, *2* (4), 366–373. DOI: 10.1038/s41929-019-0231-9.
(81) Yang, C.; Li, R.; Zhang, K. A. I.; Lin, W.; Landfester, K.; Wang, X. Heterogeneous photoredox flow chemistry for the scalable organosynthesis of fine chemicals. *Nat. Commun.* **2020**, *11* (1), 1239. DOI: 10.1038/s41467-020-14983-w.